

INFLUENCE OF AMPLITUDE AND FREQUENCY ON CUTTING FORCE AND SURFACE INTEGRITY DURING ULTRASONIC VIBRATION ASSISTED GRINDING CFRP

Y. Chen¹, Y.C. Fu²

Jiangsu Key Laboratory of Precision and Micro-Manufacturing Technology, Nanjing University of Aeronautics and Astronautics
Yudao Street 29, Nanjing, jiangsu, 210016, China

¹Email: ninaych@nuaa.edu.cn,

²Email: yucanfu@nuaa.edu.cn,

Keywords: Ultrasonic vibration assisted grinding, fiber orientation, amplitude and frequency, main cutting force, surface integrity

ABSTRACT

Ultrasonic vibration assisted grinding is one of the effective ways of machining difficult-to-cut materials. The feasibility of varying amplitude and frequency was analyzed by changing the overhang length of tool. And the effect of amplitude and frequency on the quality of machining was discussed. The experiment was conducted with single layer brazing milling tool on different orientation fiber laminate, on which diamond grains were defined distribution. The influence of amplitude and frequency on cutting force and surface integrity was analyzed, which had a certain guiding significance for choosing appropriate value. The test results show that the maximum linear velocity is the product of amplitude and frequency. The main cutting force is decreased with the increase of product of amplitude and frequency. The maximal main cutting force is obtained when the fiber orientation is 135°, while the main cutting force reaches its minimum value when the fiber orientation is 45°. The amount of broken fiber in 0° fiber orientation laminate is decreased, while the resin smearing and the fiber pull out in 45° and 90° fiber orientation laminate is decreased, while the groove in 135° fiber orientation laminate decreased with the product of amplitude and frequency increasing.

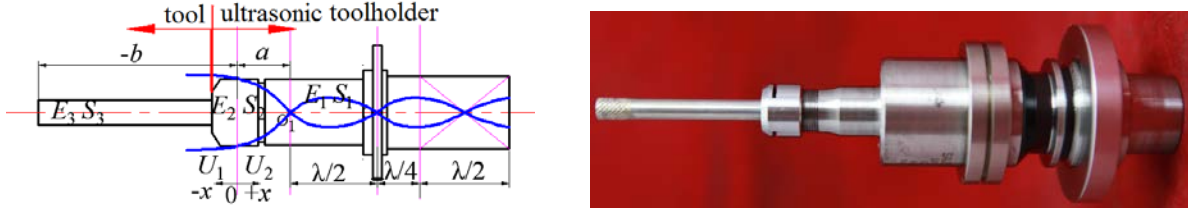
1 INTRODUCTION

The popularity of carbon fiber reinforced polymers (CFRP) in the aerospace industry has been increasing thanks to their desirable mechanical and physical properties [1]. Despite the fact that CFRP are mostly produced near net shape, machining is often required in order to bring the component into dimensional requirements and prepare it for assembly. Conventional machining processes such as milling, turning and drilling are most used for this purpose [1-2]. Due to the significant difference in mechanical properties of carbon fiber and matrix, traditional machining of carbon fiber reinforced polymer (CFRP) composite products is quite difficult. Because ultrasonic vibration assisted grinding (UAG) adds a displacement of micro-scale amplitude with an ultrasonic frequency to the tip motion of a cutting tool which consequently makes the instant depth of cut much smaller than a fiber diameter, this kind of machining methods may improve the surface integrity. So, UAG is a good method among the conventional and non-conventional machining techniques for CFRP.

In this work, to investigate the influence of amplitude and frequency on cutting force and surface integrity of different fiber orientation, ultrasonic vibration assisted grinding CFRP experiments have been carried out. First, the feasibility of changing amplitude and frequency is analyzed by changing the overhang length of tool. Then, amplitude and resonance frequency of the system at the end of the axial displacement have been changed by changing the overhang length of tool when ultrasonic vibration assisted grinding CFRP plates. Furthermore, the mechanical model of cutting forces is established by ultrasonic vibration assisted grinding four fiber orientations (0°, 45°, 90° and 135°) CFRP plates. Finally, the machined surface qualities of CFRP plates with four fiber orientations are analyzed.

2 FEASIBILITY ANALYSIS OF CHANGING AMPLITUDE

The schematic diagram and photo of tool and tool holder in ultrasonic vibration system is shown in Figure 1 (a) and (b), respectively. The position between tool and the spring clamp part is set as the origin of coordinates, while a is the distance between the origin and vibration node of ultrasonic horn, and b is the distance from the origin to the tip of the tool. S_1 is the cross-sectional area of the horn, and S_2 is the cross-sectional area in the position a , and S_3 is the cross-sectional area of tool, and o_1 is the position of the vibration node.



(a) Schematic diagram of tool and tool holder (b) Photo of the tool and tool holder

Figure 1 Picture of tool and tool holder in ultrasonic vibration system

According to the Zhu Zhemin[3], the general expression for the longitudinal vibration of a cylindrical rod with arbitrary cross section is calculated by:

$$S \frac{\partial^2 U}{\partial t^2} = c^2 \frac{\partial}{\partial x} \left(S \frac{\partial U}{\partial x} \right) \quad (1)$$

where E_1 : the elastic modulus of the horn, E_2 : the elastic modulus of position a , E_3 : the elastic modulus of tool, c : the propagation velocity of sound waves in various materials; U_1 : amplitude of tool, U_2 : amplitude of position a . The amplitude of the vibration node is 0.

The critical condition for the vibration of one end of the fixed rod is calculated by:

$$\left. \frac{\partial U}{\partial x} \right|_{x=L} = 0 \quad U(x) \Big|_{x=0} = 0 \quad (2)$$

The general solution of the given equation is calculated by:

$$U_1(x, t) = (A \cos \frac{\omega}{c} x + B \sin \frac{\omega}{c} x) \sin(\omega t + \varphi) \quad (3)$$

$$U_2(x, t) = (C \cos \frac{\omega}{c} x + D \sin \frac{\omega}{c} x) \sin(\omega t + \varphi) \quad (4)$$

According to figure 1 and formula (2), the boundary condition is:

$$x = a: \quad U_2 = 0 \quad (5)$$

$$x = 0: \quad U_1 = U_2 \quad (6)$$

$$E_3 S_3 \frac{\partial U_1}{\partial x} = E_2 S_2 \frac{\partial U_2}{\partial x} \quad (7)$$

$$x = -b: \quad \frac{\partial U_1}{\partial x} = 0 \quad (8)$$

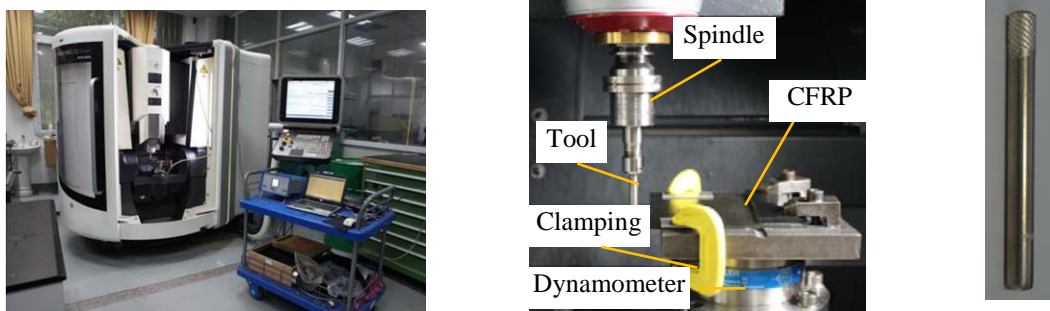
Thus, the following equation can be derived from the above equations

$$\tan\left(\frac{\omega}{c} a\right) \tan\left(\frac{\omega}{c} b\right) = \frac{E_3 S_3}{E_2 S_2} \quad (9)$$

It means that the different amplitude of the position b can be obtained by changing the length of the cutting tool.

3 EXPERIMENTAL DETAILS AND PROCEDURES

The CFRP laminates are fabricated from IMS/X850 prepregs with T800 carbon fibers. The used CFRP composite laminates is a unidirectional composite laminates and the fiber volume fraction is 65%. CFRP laminates have a thickness of 2mm. The laminates are cut into 200mm × 150mm using diamond-edged saw to fit the clamp. All grinding experiments have been carried out on a DMG Ultrasonic 20 Linear as shown in Fig. 2(a). The DMG Ultrasonic 20 Linear has maximum spindle speed of 42 000rpm and maximum feed speed of 5 m/min. The experimental data are collected with a data acquisition system composed of a 9272 Kistler dynamometer and a 5070A Kistler amplifier. The amplitude is measured by the M70LL/0.5 ultra high speed laser displacement sensor, and the sampling frequency of the laser displacement sensor is 100 kHz. The fixation of the composite material laminate is made as shown in Fig. 2(b), to make sure that vibrations and displacement are eliminated. The brazed diamond tool has been employed to avoid the effect of tool wear on the cutting force as shown in Fig.2(c) and the tool parameters is shown in table 1.



(a) The experimental equipments (b) Fixation of the composite material (c) Brazed diamond tool

Figure 2 The experimental setup

Material	Diameter (mm)	Length (mm)	Size (μm)	Brazing alloy	Helix angle	Rows
0Cr18Ni9	6	60	140-150	Ag-Cu-Ti	45°	16

Table 1: Brazed diamond tool parameters.

A multivariate factor method for two factors (amplitude A and frequency f) is used for the elaboration of the plan of experiments. The UAG tests are executed at spindle speed of 8000 rpm, and feed rate of $4\mu\text{m}/\text{z}$ and Table 2 indicates in detail all factors studied. 4% volume fraction of Castrol Syntilo 9954 water-based emulsion is adopted as Cutting fluid. The test of different parameter combinations are replicated three times.

n ($\text{r}\cdot\text{min}^{-1}$)	f_z ($\mu\text{m}\cdot\text{z}^{-1}$)	a_e (μm)	a_p (mm)	A (μm)	f (KHz)
8000	4	400	2	7	20.6
				6	21.1
				5.5	23.1
				5	20.5
				0	0

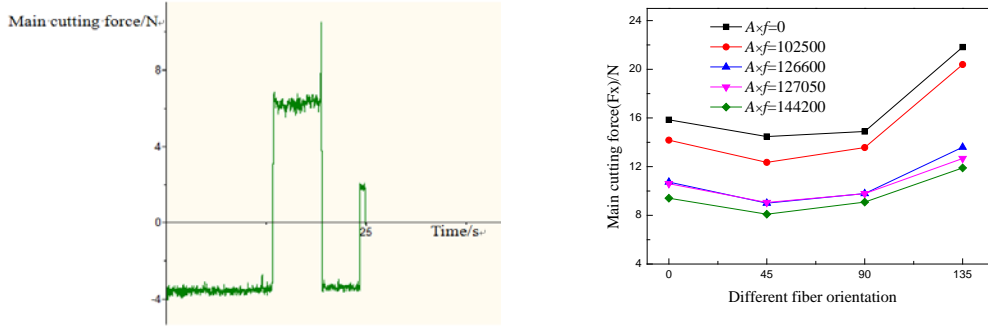
Table 2 Test parameters.

After machining, the workpieces are observed through digital microscope HIROX KH-7700 and SEM (scanning electron microscope) Hitachis-3400N II.

4 RESULTS AND DISCUSSION

4.1 Cutting force

Fig. 3 (a) displays the measured main cutting force (F_x) when fiber direction angle is 0° . Fig. 3 (b) displays the measured main cutting force (F_x) as a function of fiber direction angle and the product of amplitude and frequency.



(a) Cutting force diagram (fiber direction angle 0°) (b) Cutting force in different fiber directions

Figure 3: Variation trend of main cutting forces (F_x) with different fiber directions

The value of main cutting force is the smallest in the fiber direction of 45° , and the biggest cutting force is in the fiber direction of 135° as shown in the figure 3 (b). The value of main cutting force in the fiber direction of 0° is similar to that in the fiber direction of 90° . The reason is that the fracture mode of the material is different in the different fiber directions.

With the increase of the product of amplitude and frequency, main cutting force decreases in all fiber directions as shown in the figure 3 (b). This is mainly due to the increase of the product of frequency and amplitude, the rake angle become smaller in the UAG machining process.

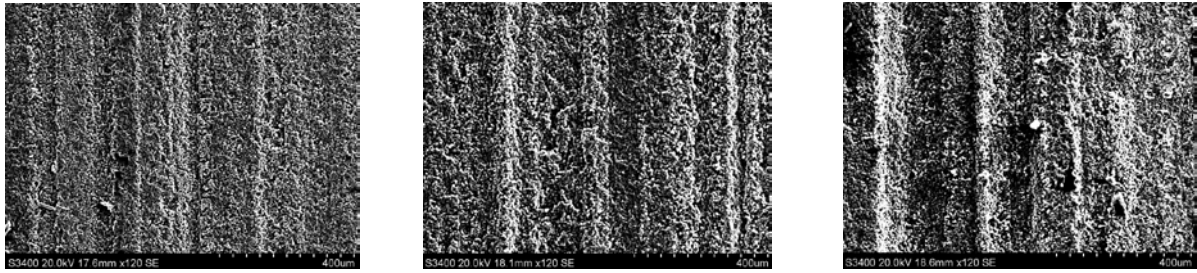
4.2 Machined Surface Quality of CFRP

Machined surface topographies with various products of amplitude and frequency for 4 kinds of fiber direction angles (0° , 45° , 90° and 135°) are as shown in Figure 4 - Figure 7. It can be found in figure 4 (c) that there are many broken chip and machined surface is a rough surface, which there is a compression force on the fibers mainly due to the negative rake angle of diamond particles when the CFRP is machined by brazed diamond tool. Compared with figure 4 (c), the machined surfaces in figure 4 (a) and figure 4 (b) are much smoother. The reasons are that UAG process can improve the sharpness of tools so that cutting process is more smoothly on the one hand. On the other hand, there exists a certain degree of ultrasonic cleaning and ultrasonic cavitation between the tool and workpiece surface because of the role of cutting fluid. Furthermore, with the increase of the product of amplitude and frequency, machined surface in figure 4 (a) is smoother than that in figure 4 (b). Due to with the increase of the product of amplitude and frequency, the sharpness of tools is improved significantly.



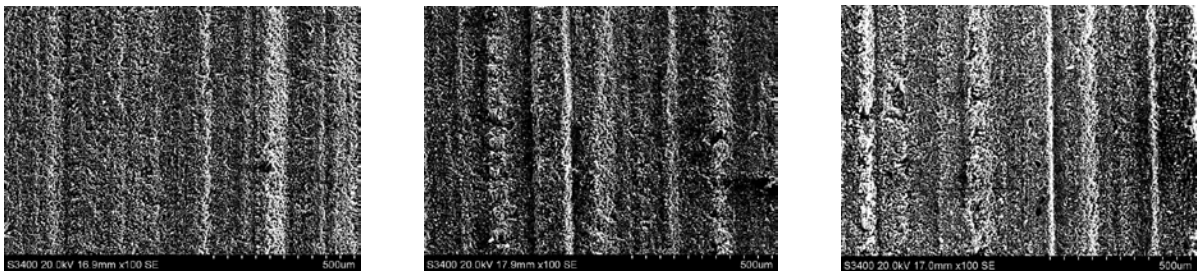
(a) $A=7\mu\text{m}$ $f=20.6\text{KHz}$ $A \times f=144200$ (b) $A=5\mu\text{m}$ $f=20.5\text{KHz}$ $A \times f=102500$ (c) $A=0$ $f=0$ $A \times f=0$

Figure 4: Surface topographies with various products of amplitude and frequency (fiber direction angle 0°)



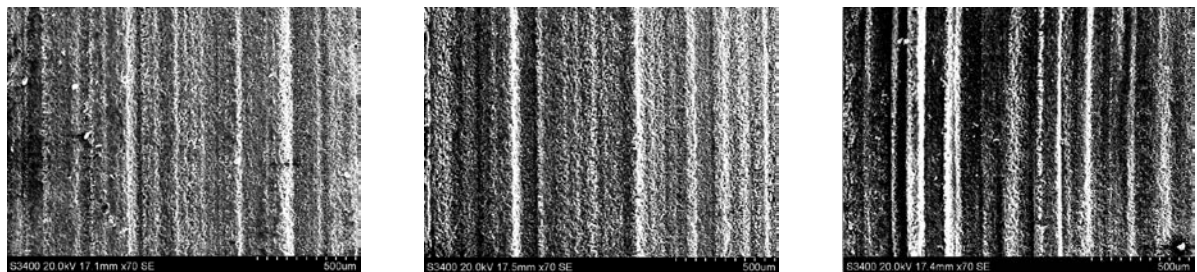
(a) $A=7\mu\text{m}$ $f=20.6\text{KHz}$ $A \times f=144200$ (b) $A=5\mu\text{m}$ $f=20.5\text{KHz}$ $A \times f=102500$ (c) $A=0$ $f=0$ $A \times f=0$

Figure 5: Surface topographies with various products of amplitude and frequency (fiber direction angle 45°)



(a) $A=7\mu\text{m}$ $f=20.6\text{KHz}$ $A \times f=144200$ (b) $A=5\mu\text{m}$ $f=20.5\text{KHz}$ $A \times f=102500$ (c) $A=0$ $f=0$ $A \times f=0$

Figure 6: Surface topographies with various products of amplitude and frequency (fiber direction angle 90°)



(a) $A=7\mu\text{m}$ $f=20.6\text{KHz}$ $A \times f=144200$ (b) $A=5\mu\text{m}$ $f=20.5\text{KHz}$ $A \times f=102500$ (c) $A=0$ $f=0$ $A \times f=0$

Figure 7: Surface topographies with various products of amplitude and frequency (fiber direction angle 135°)

The same conclusions can be derived from figure 5 to figure 7 that machined surfaces become smoother with the increase of the product of amplitude and frequency. However, fiber orientation has a decisive influence on the surface morphology. Machined surfaces oriented at 45° suffered severe damage where fibers are generally bent and lifted-up as the cutting edge advanced, which can subsequently cause splitting or interfacial failure of fiber bundles and the matrix. Some of these fibers then proceeded to fracture/were pulled out while others were merely flexed, thereby producing a wavy surface. Machined surfaces with fibers at 0° generally showed the least damage, with fibers removed cleanly as a result of fracture by buckling [4]. Fiber pull out was observed in 90° and 135° machined surfaces leading to empty holes or large grooves as fibers tended to break at locations beneath the machined surface/depth of cut [5]. The softened matrix allows flexible fibers to escape from the cutting edge and spread over a wider area, especially those in the 90° and 135° direction.

5 CONCLUSIONS

Based on the results obtained from the experiments, the following conclusions could be extracted.

(1) By the effect of the tool overhang lengths on amplitude and frequency analyzing, the different amplitudes and frequencies can be achieved by changing the tool overhang lengths.

(2) The main cutting force (F_x) decreases with increase of the product of amplitude and frequency in UAG process of CFRP, and $F_x(135^\circ) > F_x(0^\circ) > F_x(90^\circ) > F_x(45^\circ)$.

(3) Machined surfaces become smoother with the increase of the product of amplitude and frequency in all fiber directions. However, fiber orientation has a decisive influence on the surface morphology.

ACKNOWLEDGEMENTS

The authors gratefully acknowledge the financial support received from the National Nature Science Foundation of China (No. 51375234), Jiangsu Key Laboratory of Precision and Micro-Manufacturing Technology and Liaoning Province Natural Science Foundation of China (Aviation joint fund, No. 2014028024).

REFERENCES

- [1] Y. Karpat, O. Bahtiyar and B. Değer, Mechanistic force modeling for milling of unidirectional carbon fiber reinforced polymer laminates, *International Journal of Machine Tools and Manufacture*, 56, 2012, pp. 79-93.
- [2] J.Y. Sheikh-Ahmad, *Conventional Machining Operations*, Machining of polymer composites, Springer, New York, 2009.
- [3] Z. Zhu, X. Gong, G. Du. Acoustic Base. Nanjing University Press, Nanjing, 2001.
- [4] F. Klocke, W. König, S. Rummenholler, and C. Wurtz, In: *Machining of ceramics and composites*, edited by S. Jahanmir, M. Ramulu, P. Koshy Marcel Dekker Publishing, New York 1999, pp 249-266
- [5] H.Y. Puw, and H. Hocheng, In: *Machining of ceramics and composites*, edited by S. Jahanmir, M. Ramulu, P. Koshy Marcel Dekker Publishing, New York 1999, pp 267-294